Edited by H. Ryssel, P. Pichler - September 1995

An Accurate NMOS Mobility Model for 0.25μm MOSFETs

S. A. Mujtaba[a,b], M. R. Pinto[b], D. M. Boulin[b], C. S. Rafferty[b], R. W. Dutton[a]

[a]Center for Integrated Systems, Stanford University
Stanford, California 94305, USA

[b]AT&T Bell Laboratories
Murray Hill, New Jersey 07974, USA

Abstract

A physically-based, semi-empirical, local mobility model for 2D device simulation is presented that is accurate in both the intrinsic (channel) as well as the extrinsic (parasitic) regions of LDD MOSFETs. It is demonstrated that for deep submicron MOSFETs the gate-voltage-dependent extrinsic series resistance is poorly modeled by existing mobility models. A systematic methodology is presented for the calibration and validation of the new model with experimental data. Broad applicability of the new model is established with excellent agreement for a range of experimental data (subthreshold, linear, and saturation) including channel lengths from 20.0μm down to 0.25μm.

1. Introduction

The various components that contribute to resistance in an LDD MOSFET include inversion-layer resistance (which occurs in the channel), accumulation-layer resistance (which occurs in the overlap region between the gate and the LDD diffusion), spreading resistance (which occurs near the end of the accumulation layer owing to current crowding), bulk sheet resistance, and contact resistance. As MOSFET dimensions continue to scale, reductions in channel length and oxide thickness have led to a decrease in the inversion-layer resistance. However, hot-carrier reliability concerns have not allowed the LDD resistance to scale proportionally with channel resistance.

Traditionally, channel resistance was the dominant factor limiting current transport in a MOSFET. Naturally, most of the effort was devoted to modeling mobility in the inversion layer. This is no longer the case in deep submicron MOSFETs which tend to have non-negligible LDD resistance; simulations that use conventional mobility models whose formulation is based only on the inversion-layer over-predict the drain current and fail to capture the slope of the I_d-V_{gs} curve as well. Figure 1 illustrates this point for a 0.25μm MOSFET. Although the value of the contact resistance (which is obtained experimentally) is supplied to the simulator, incorrect calculation of mobility in the accumulation-layer leads to significant errors in the I-V curves.

To address the above concerns, we present a new mobility model that accurately models both the accumulation and inversion layer components. For purposes of calibrating the new model with experimental data, we present a systematic methodology that involves coupled process and device simulations, and emphasizes the need for extraction of parameters from standard test structures that are critical for benchmarking of mobility. We demonstrate broad applicability of the model by presenting excellent agreement between simulation and experimental data for devices from 20μm down to 0.25μm.

2. New Model

The new model builds upon earlier work that treated inversion-layer mobility in a comprehensive fashion [1]. The distinguishing features between this new model and the earlier work is the treatment of various scattering mechanisms in the 2D accumulation layer. Figure 2 illustrates how the new model is partitioned based on the "dimensionality" and the nature of the scattering mechanisms.

It was experimentally shown by Sun and Plummer [2] that both the accumulation-layer and inversion-layer electrons follow the same universal mobility curve (UMC). Since the model reported in our previous work was calibrated using the UMC, it provides a natural platform for extension to the accumulation layer. The model for inversion-layer phonon scattering has a channel-doping-dependent term, which is required in order to reproduce all the properties of the UMC. To extend this model to the accumulation layer, the doping dependence is modified to account for both donors (which occur in the accumulation layer) and acceptors (which occur in the inversion-layer). Thus, the model for 2D phonon scattering is given by:

$$\mu_{ph}^{2D} = \frac{A}{E_{\perp}} + \frac{B\,(N_A + N_D)^{\gamma}}{T \cdot E_{\perp}^{1/3}} \tag{1}$$

Fundamentally, Coulombic scattering in the inversion layer differs from that in the accumulation layer because attractive charge centers (donors) are more effective in scattering electrons than repulsive charge centers (acceptors). The ratio of attractive to repulsive Coulombic mobility has been modeled by Klaassen [3], and it appears as the function *G(P)* in Klaassen's formulation. Inversion-layer Coulombic mobility, which was modeled in our previous work [1], is scaled with *G(P)* to obtain the accumulation-layer Coulombic mobility, as shown below:

$$\mu_{acc}^{2D} = \left[\mu_{inv}^{2D}(N_A{=}N_D)\right] \cdot G(P) \text{ where } \mu_{inv}^{2D} = max\left[D_1 \frac{n^{\kappa}}{N_A^{\nu}}, \frac{D_2}{N_A^{\upsilon}}\right] \tag{2}$$

In the case of surface roughness scattering, the model for the inversion layer also applies to the accumulation layer unless the accumulation-layer interface is known to be different from that of the inversion-layer. Hence, the following expression holds for both the accumulation and the inversion layer:

$$\mu_{sr} = C/E_{\perp}^{2} \tag{3}$$

Total phonon scattering is obtained by taking the *minimum* of 2D phonon and 3D phonon scattering, where 3D phonon scattering is given by:

$$\mu_{ph}^{3D} = \mu_{max} \cdot \left[\frac{300}{T}\right]^{\theta} \tag{4}$$

2D Coulombic mobility is given by the Matthiessen's sum of accumulation-layer and inversion-layer mobility given in (2). To get the total Coulombic mobility, the 2D term and the 3D term are pieced together through a transition function:

$$\mu_C = f(\alpha)\,\mu_C^{3D} + [1 - f(\alpha)]\,\mu_C^{2D} \text{ where } \alpha = \alpha(E_{\perp}) \tag{5}$$

and the 3D term for Coulombic mobility is taken from [3].

Total transverse field mobility is obtained via a Matthiessen's summation of phonon,

surface roughness, and Coulombic scattering. The transverse field model is coupled with Hansch's [4] longitudinal-field degradation model to arrive at the complete model.

Compared with our earlier model for inversion-layer electrons [1], no new calibrating parameters are introduced in the formulation of the new model, since the extension from the earlier model has been performed on a physical basis.

3. Validation Methodology

In order to compare the new mobility model with experimental data obtained from *actual* devices that have highly non-uniform doping profiles, the validation procedure necessarily requires coupled process and device simulations. The outline of the validation procedure is shown in Fig. 3. The first step is to supply the process recipe to AT&T's process simulator, PROPHET, which then generates 2D doping and geometry information. Before any I-V curves can be generated by the device simulator using the new model, it needs to be supplied with the values for effective oxide thickness ($T_{ox,eff}$) and contact resistance (R_{co}). $T_{ox,eff}$ is obtained from low-frequency C-V rather than ellipsometric measurements since quantum and poly-depletion effects invariably make electrical thickness to appear larger than the physical thickness. R_{co} is calculated from measurements made on 4-probe Kelvin test structures.

After the specification of the device structure is complete, the validation methodology proceeds in a step-wise manner. First, the linear I-V characteristics of a long channel device (20μm) are compared with device simulations to validate the accuracy of the inversion-layer part of the model. Next, the linear I-V characteristics of the short channel devices are examined. Fig. 4 illustrates that excellent agreement is obtained in the linear region across four short channel devices. On comparison with Fig. 1, Fig. 4 confirms that the accumulation-layer mobility is modeled accurately. At this stage, the transverse-field part of the model has been conclusively established, the next step is to examine the model in saturation. As Fig. 5(a) and (b) illustrate, the model provides excellent fits in saturation as well for devices ranging from 20μm to 0.25μm, thus establishing broad applicability and accuracy of the model over a wide range of channel lengths.

4. Conclusions

We have presented a new MOSFET mobility model for 2-D device simulation that is accurate in both inversion and accumulation layers. Based on a systematic calibration methodology, we demonstrated broad applicability of the new model by showing excellent agreement with data over a wide range of channel lengths down to 0.25μm.

5. Acknowledgments

This work was supported by AT&T Bell Labs and the Semiconductor Research Corporation. The authors gratefully acknowledge the help of Stephen Moccio in I-V measurements, and thank Kathleen Krisch for providing C-V data.

6. References

[1] S. A. Mujtaba et. al., *NUPAD-IV*, Honolulu, Hawaii, June 5-6, 1994, pp. 3-6
[2] S. C. Sun and J. D. Plummer, *IEEE Trans. Elec. Dev.*, vol. 27, p. 1497, 1980
[3] D. M. B. Klaassen, *Solid State Electronics*, vol. 35, no. 7, pp. 953-959, 1992
[4] W. Hänsch and M. Miura-Mattausch, *NASECODE-IV*, Dublin, 1985

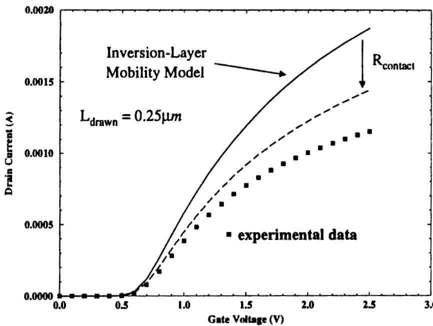

Figure 1. Mobility models formulated for the inversion-layer incorrectly calculate mobility in the accumulation layer, leading to significant errors in I-V curves in the case of deep submicron LDD MOSFETs, which have non-negligible accumulation-layer resistance.

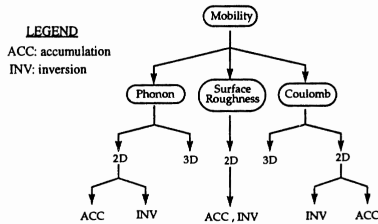

Figure 2. Mobility model hierarchy illustrating the scope of the new model. Essential features of the new model include the addition of the accumulation terms.

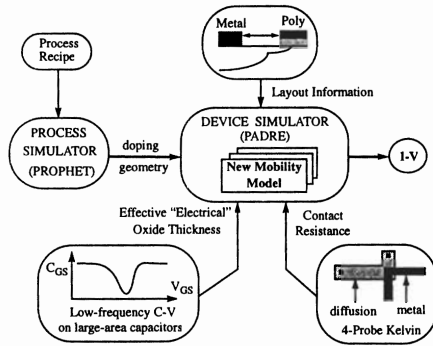

Figure 3. Validation Methodology involves coupled process and device simulations. The process recipe is fed to the process simulator to get the 2D doping profiles. Effective oxide thickness and contact resistance values are supplied to the device simulator from independent measurements. Together with the layout information, simulations are performed with the new model to generate I-V curves, which are then compared with experimental data from devices fabricated based on the process recipe.

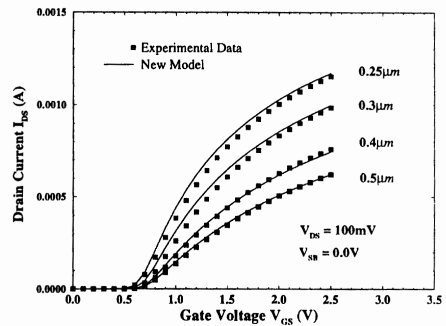

Figure 4. Comparison between the new mobility model and experimental data across four short channel devices is presented, establishing the accuracy of the new model.

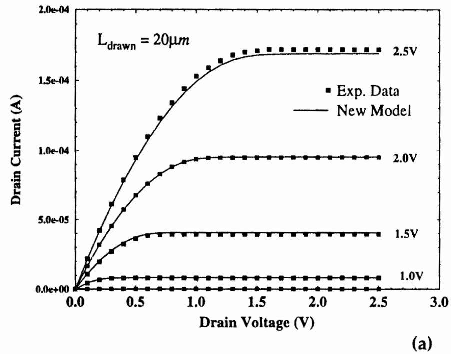

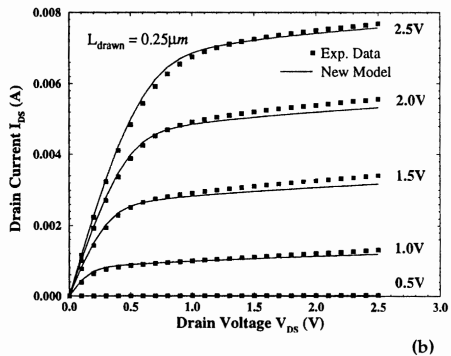

Figure 5. Broad applicability of the new model is also demonstrated in saturation, where comparison between the new model and experimental data is shown for a 20μm and a 0.25μm device. Channel lengths between 20 and 0.25μm exhibit excellent fits as well.